Luminescence

WILEY

LUMINESCENCE
The Journal of Biological and Chemical Luminescence

RESEARCH ARTICLE

Structure and Luminescence Properties of Novel $Dy^{3+}$and Tb^{3+} Activated $Ca_{10}(PO_4)_6Cl_2$ Phosphors for Solid-State Lighting Devices

Roshana. T. Maske[1] | A. N. Yerpude[1] | Rupesh. S. Wandhare[2] | D. M. Parshuramkar[1] | N. R. Pawar[2]

[1]Department of Physics, N.H. College, Chandrapur, India | [2]Department of Physics, ACS College, Yavatmal, India

Correspondence: A. N. Yerpude (atulyerpude@gmail.com) | Rupesh. S. Wandhare (rwandhare1994@gmail.com)

Received: 19 March 2025 | **Revised:** 10 June 2025 | **Accepted:** 14 June 2025

Funding: The authors received no specific funding for this work.

Keywords: Dy^{3+} ions | phosphor | PL | SEM | Tb^{3+} ions | wet chemical technique

ABSTRACT

The novel Dy^{3+}-and Tb^{3+}-doped $Ca_{10}(PO_4)_6Cl_2$ phosphor is synthesized by the conventional wet chemical technique. The XRD pattern of prepared Dy^{3+} and Tb^{3+} doped in host material is in well agreement with the PDF card no. 7032212. The SEM image shows that the size of the particle is non-uniform in size and shape; it ranges in submicrometers. FTIR analysis confirms phosphate $(PO_4)^{3-}$ and Ca-O group bonding present in $Ca_{10}(PO_4)_6Cl_2$ phosphor. The photoluminescence spectra of the prepared $Ca_{10}(PO_4)_6Cl_2$:Dy^{3+} phosphor, under the excitation at 350 nm, it exhibit two emission peaks located at 474 nm ($^4F_{9/2} \rightarrow {}^6H_{15/2}$) and 572 nm ($^4F_{9/2} \rightarrow {}^6H_{13/2}$), emitting blue and orange color respectively. The high-intensity peak is located at 474 nm. The PLE spectra of $Ca_{10}(PO_4)_6Cl_2$:Tb^{3+} phosphor contain two strong emission peaks centered at 470 (blue) nm and 543 (green) nm, these ascribed due to $^5D_4 \rightarrow {}^7F_6$ & $^5D_4 \rightarrow {}^7F_5$ transition of Tb^{3+} ions monitored at 354 and 379 nm excitation. The concentration quenching mechanism between the Dy^{3+}–Dy^{3+} ions and Tb^{3+}-Tb^{3+} ions is primarily attributed to dipole–dipole (d–d) interactions. The results suggest that $Ca_{10}(PO_4)_6Cl_2$:RE (RE = Dy^{3+}, Tb^{3+}) phosphor shows promise for use as a near-UV phosphor in solid-state lighting applications.

1 | Introduction

Over the past decade, nanophosphors, which are solid inorganic materials, have gained popularity among researchers because of their unique physical property, chemical property, and optical property. WLEDs (White light-emitting diodes) are highly sought after the solid-state lighting (SSL) technologies as a substitution for fluorescent and traditional lights [1–3]. There are two techniques to create white light from LEDs. One approach is by combining different colored lights from multiple LED chips, known as multichip LEDs. The second method is using phosphors for conversion of blue or ultraviolet (UV) LED light into longer wavelengths, called phosphor-converted LEDs (pc-LEDs) [4, 5]. Inorganic phosphor activated by rare earth ions has attracted significant curiosity because of its different applications, such as in fluorescent lighting, biological labeling, solid-state lasers, white LEDs, and display devices [6–8]. In recent decades, researchers have studied various rare earth-doped materials. The visible light emission from these doped phosphors makes them useful in many fields.

Phosphate phosphors are widely used due to their superior thermal stability and great brightness, and customizable emission colors. Phosphate phosphors, made from combine with phosphorus, oxygen, and another elements, have several benefits. They are very bright, stable at high temperatures, and can emit different colors of light. These properties make them ideal for applications in lighting devices, like LED bulbs and

fluorescent lamps, also in display technologies like screens and monitors. Additionally, their compatibility with various light sources and stable performance under different conditions make them suitable for medical imaging and diagnostic tools. The versatility and efficiency of phosphate phosphors continue to drive their use in both everyday and specialized technologies [9–12]. Among all rare earth ions, Dy^{3+}-activated phosphor materials are particularly interesting because of their parity and spin-allowed 4f-5d optical transitions, which exhibit a rapid emission lifetime of approximately 10–50 ns [13].

Dy^{3+} ions play a crucial role in producing yellow color light in luminescent materials. They exhibit two main emission bands: yellow light at 550–600 nm from the $^4F_{9/2} \rightarrow {}^6H_{13/2}$ transition and blue light at 460–500 nm from the $^4F_{9/2} \rightarrow {}^6H_{15/2}$ transition [14]. The blue light emission is due to the magnetic dipole (MD) transition, which is stable across different crystal fields. In contrast, the yellow light emission comes from an electric dipole (ED) transition and is highly affected by the chemical surroundings around the Dy^{3+} ions [15].

C. Nandanwar et al. [14] stated that Dy^{3+}- and Eu^{3+}-doped $NaSrPO_4$ phosphors were prepared by wet chemical synthesis; the Dy^{3+} ion emission band was found at 519 and 613 nm for wLEDs. Dy^{3+}- and Eu^{3+}-doped $Ca_3(PO_4)_2$ phosphor was preapred by using wet chemical synthesis; the Dy^{3+} ion emissions were found at wavelengths 483 nm and 574 nm for SSL. Dy^{3+}-doped $Ba_2Ca(PO_4)_4$ phosphor was prepared by the wet chemical route [15]. S. Morya et al. [16] discussed KCa $(PO_3)_3$:Dy^{3+} phosphors was produced by utilizing solid-state reaction (SSR) synthesis and wavelength of emission at 575 nm to produce high-quality w-LEDs and photonic applications. The Dy^{3+}-doped $NaCaPO_4$ phosphor prepared through combustion method and wavelength of emission blue at 482 nm, and yellow at 576 nm for white-LEDs and another solar applications [17]. $LaPO_4$: Dy^{3+} phosphor sample is synthesized by wet chemical synthesis method, emission at 435 nm [18]. Dy^{3+}-doped $LiSrP_3O_9$ phosphors are prepared by using a combustion route. The different emission peaks position at 476, 570, and 657 nm for wLEDs [19]. $KZnPO_4$:RE (RE = Dy^{3+}, Sm^{3+}) phosphors are synthesized through Combustion technique. The emission peaks located at 562 nm and 597 nm for near-UV region for w-LEDs [20]. B. Ramesh et al. [21] stated green emitting Tb^{3+}-doped $CaZn_2(PO_4)_2$ phosphors was produced by SSR route and emission peak at high intensity at 542 nm. Dy^{3+}-, Tb^{3+}-, and Sm^{3+}-doped $BiPO_4$ phosphors were produced through wet chemical synthesis, and Dy^{3+} phosphor shows emission at 481 nm ($^4F_{9/2} \rightarrow {}^6H_{15/2}$) and 575 nm ($^4F_{9/2} \rightarrow {}^6H_{13/2}$). Tb^{3+} ion phosphor emission wavelength at 545 nm ($^5D_4 \rightarrow {}^7F_5$) shows narrow green emission [22]. The $Sr_2P_2O_7$: Tb^{3+} phosphor synthesized through co-precipitation route and intense emission peak at $^5D_4 \rightarrow {}^5F_5$ (543 nm) [23]. The green emitting $NaCaPO_4$:Tb^{3+} phosphor was prepared by SSR method it shows strong emission band at 547 nm for SSL applications [24]. The X-ray diffraction of $Ca_{10}(PO_4)_6Cl_2$ phosphor host material is already published in my previous research paper [25].

This work investigates the luminescence characteristics of Dy^{3+} and Tb^{3+}doped $Ca_{10}(PO_4)_6Cl_2$ phosphor produced by wet chemical synthesis The crystal structure, stretching modes, morphological structure, and optical properties analysis were analyzed by Vesta Software, Fourier transform infrared (FTIR) spectra, scanning emission microscopy (SEM), and photoluminescence characterization, respectively.

2 | Experimental Section

The $Ca_{10}(PO_4)_6Cl_2$:Dy^{3+} phosphor with various concentrations of Dy^{3+} ions ranging from 0.005, 0.01, 0.015, 0.02, and 0.025 was prepared through a wet chemical synthesis. The starting materials used for synthesis are ammonium dihydrogen phosphate, calcium nitrate, dysprosium oxide, and ammonium chloride, which are correctly weighed in stoichiometric ratio. All these materials are weighed by a monopan electronic balance. All these materials used have AR quality. Initially, the dysprosium oxide (RE) is in oxide form, so it transformed into nitrate by using nitric acid. Dy_2O_3, a rare earth (RE) material, is dissolved in a solution of nitric acid, which is diluted by distilled water. Then, the solution is placed on the magnetic hot plate at a low temperature of 100°C; the solution has transformed into a colorless solution. All the weighed materials are shifted to a 100mL glass beaker and mixed with each solution in distilled water, which is 20 mL, and stirred for approximately 30 min. All these solutions are then shifted to a single large beaker of about 250 mL and agitated with a magnetic stirrer for about 30 min. The solution is stirred on a heated magnetic plate at 80°C for 6 to 8 h. This results in the formation of a white powder. The obtained product was ground with a mortar and pestle to produce a fine powder. This powder was then placed in a crucible and heated in a furnace at 600°C for 4 h for annealing. Once it cooled to room temperature, the sample was ground again into a fine powder for further measurements. Similarly, the same processes were used for the preparation of Tb^{3+}-activated $Ca_{10}(PO_4)_6Cl_2$ phosphor. XRD pattern analysis was conducted using a Rigaku MiniFlex X-ray diffractometer with a scanning range of $2\theta = 10°$ to 80° and a step width of 0.02% The surface morphology was examined using a scanning electron microscope (SEM, Hitachi S-3400N). The photoluminescence excitation and PL emission spectra, in addition to all luminescence studies, were obtained using a Shimadzu RF5301 PC Spectro-fluorophotometer.

3 | Results and Discussion

3.1 | XRD Analysis of Dy^{3+}- and Tb^{3+}-Activated $Ca_{10}(PO_4)_6Cl_2$ Phosphor

The X-ray diffraction pattern of prepared sample Dy^{3+} and Tb^{3+} doped in $Ca_{10}(PO_4)_6Cl_2$ phosphor sample is displayed in Figure 1. The XRD pattern was recorded in the range $20^0 < 2\theta < 80^0$ for prepared phosphor. The X-ray pattern of synthesized Dy^{3+} and Tb^{3+} doped in $Ca_{10}(PO_4)_6Cl_2$ sample was well match with the standard PDF card no. 7032212. Figure 1 shows that the obtained result of synthesized Dy^{3+} and Tb^{3+} activated in host sample was in pure form. There is no additional or extra impurity peaks found in the XRD spectra. All diffracted peaks of prepared sample were very sharp and intense, so the end product phosphor was in homogeneous form and crystalline in nature. The obtained sample are visually ensured and physically stable.

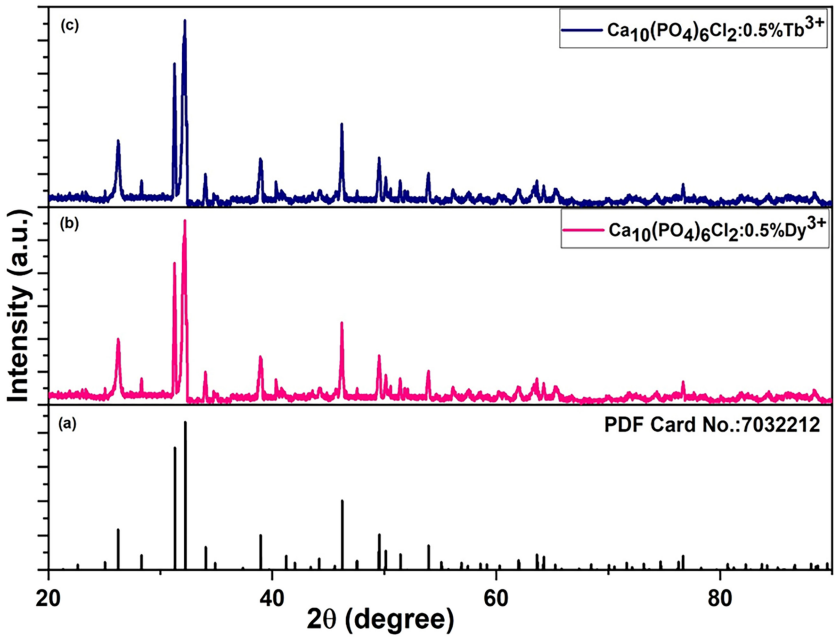

FIGURE 1 | X-ray diffraction of Dy^{3+}- and Tb^{3+}-activated $Ca_{10}(PO_4)_6Cl_2$ phosphor.

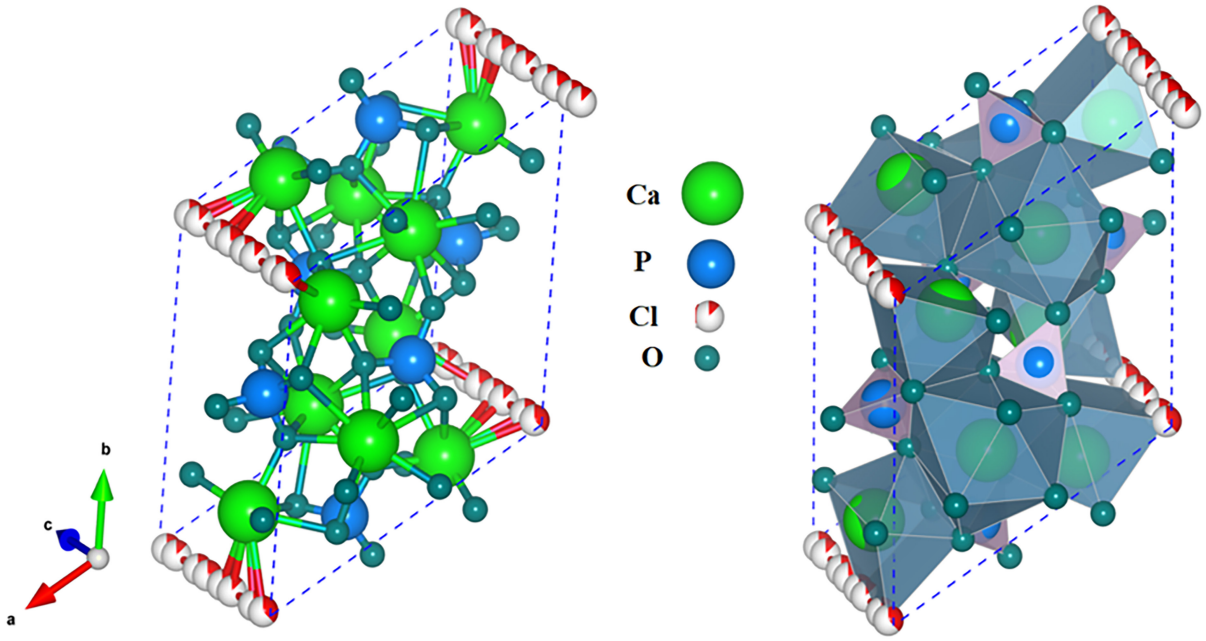

FIGURE 2 | 3D view crystal structure of $Ca_{10}(PO_4)_6Cl_2$ phosphor.

3.2 | Crystal Structure

The 3D visualization of the crystal structure of $Ca_{10}(PO_4)_6Cl_2$ phosphor is depicted in Figure 2. The typical crystal structure of $Ca_{10}(PO_4)_6Cl_2$ phosphor is obtained by using "Vesta Software". The crystal structure shows that the green color sphere represents the Ca atom. The phosphor atoms are represented by blue color spheres in crystal structure. The Cl atoms are represented in white color spheres, and the oxygen anions are represented by peacock blue color spheres. The crystal structure of synthesized $Ca_{10}(PO_4)_6Cl_2$ phosphor reveals a hexagonal phase; it is of crystalline nature with the P 63/m space group, and the lattice parameters of host $Ca_{10}(PO_4)_6Cl_2$ phosphor are $a = 9.5902$ Å, $b = 9.5902$ Å, and $c = 6.7666$ Å. The number of distinct elements is 4 ($Z = 1$), and the angles are $\alpha = 90°$, $\beta = 90°$, and $\Upsilon = 120°$. The cell volume of $Ca_{10}(PO_4)_6Cl_2$ phosphor is 538.96 $Å^3$.

3.3 | Fourier Transferred Infrared Spectroscopy

FTIR spectroscopy was used to determine the vibrations and function group contained in the sample. Figure 3 shows the

FTIR spectra of $Ca_{10}(PO_4)_6Cl_2$ phosphor, sintered at 600°C. Wavenumbers in the spectrum ranged in 4000 to 400 cm^{-1} at ambient temperature. the Optimum bandwidth was obtained at 3572.19 cm^{-1}, which is caused by the stretching (O-H) vibration of H_2O acquired by the phosphor. The vibration band at 1082.99 cm^{-1} is due to the asymmetric stretching phosphate $(PO_4)^{3-}$ group. All bands are result of the antisymmetric vibrations of stretching unbound O-H bonds. Peak measured at 1479.75 cm^{-1} is corresponding to vibrations of C-O. Figure 2 shows several absorption bands were observable in a range between 830 and 400 cm-1 because of the phonon energy associated with metal-oxygen vibrations [26].

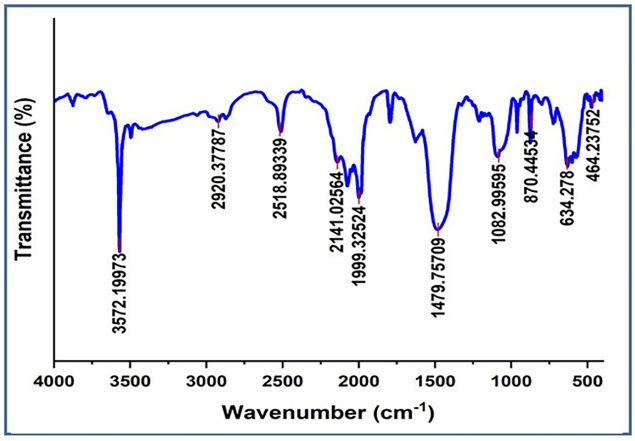

FIGURE 3 | FTIR of $Ca_{10}(PO_4)_6Cl_2$ phosphor.

3.4 | SEM

The morphological behavior of the prepared phosphor was analyzed by using SEM. Figure 4 clearly shows SEM images of the synthesized $Ca_{10}(PO_4)_6Cl_2$ phosphor at different magnifications. The analysis of SEM image confirmed that the synthesized phosphor sample has a high particle density and an agglomeration size in the micrometer range. The microstructure of materials influence its physical properties and behavior, making it possible to customize specific properties through microstructure. Utilizing micro-sized particle can enhance the photoluminescence properties of synthesized phosphor, so it is suitable for LED fabrication. Additionally, the smaller particle size facilities easier coating of the powder into LEDs. The particles appear nonuniform in nature and irregular in shape and size likely due to agglomeration and mechanical grinding during sintering.

3.5 | Photoluminescence Properties of Dy^{3+} Ions Activated in $Ca_{10}(PO_4)_6Cl_2$ Phosphor

Figure 5 shows the photoluminescence spectra of Dy^{3+}-activated $Ca_{10}(PO_4)_6Cl_2$ phosphor, monitored at constant optimum wavelength of emission at 474 nm. The PLE spectrum range 300–400 nm wavelength. The photoluminescence excitation spectra contain four absorption peaks at 325, 350, 365, and 389 nm, which corresponds to characteristic peaks of $^6H_{15/2} \rightarrow {}^5F_{5/2}$, $^6H_{15/2} \rightarrow {}^6P_{7/2}$, $^6H_{15/2} \rightarrow {}^4I_{11/2}$, and $^6H_{15/2} \rightarrow {}^4I_{3/2}$ transition of Dy^{3+} ions, respectively [27, 28]. Among all various excitation peaks, the most intense peaks observed at 350 mm. These suggest

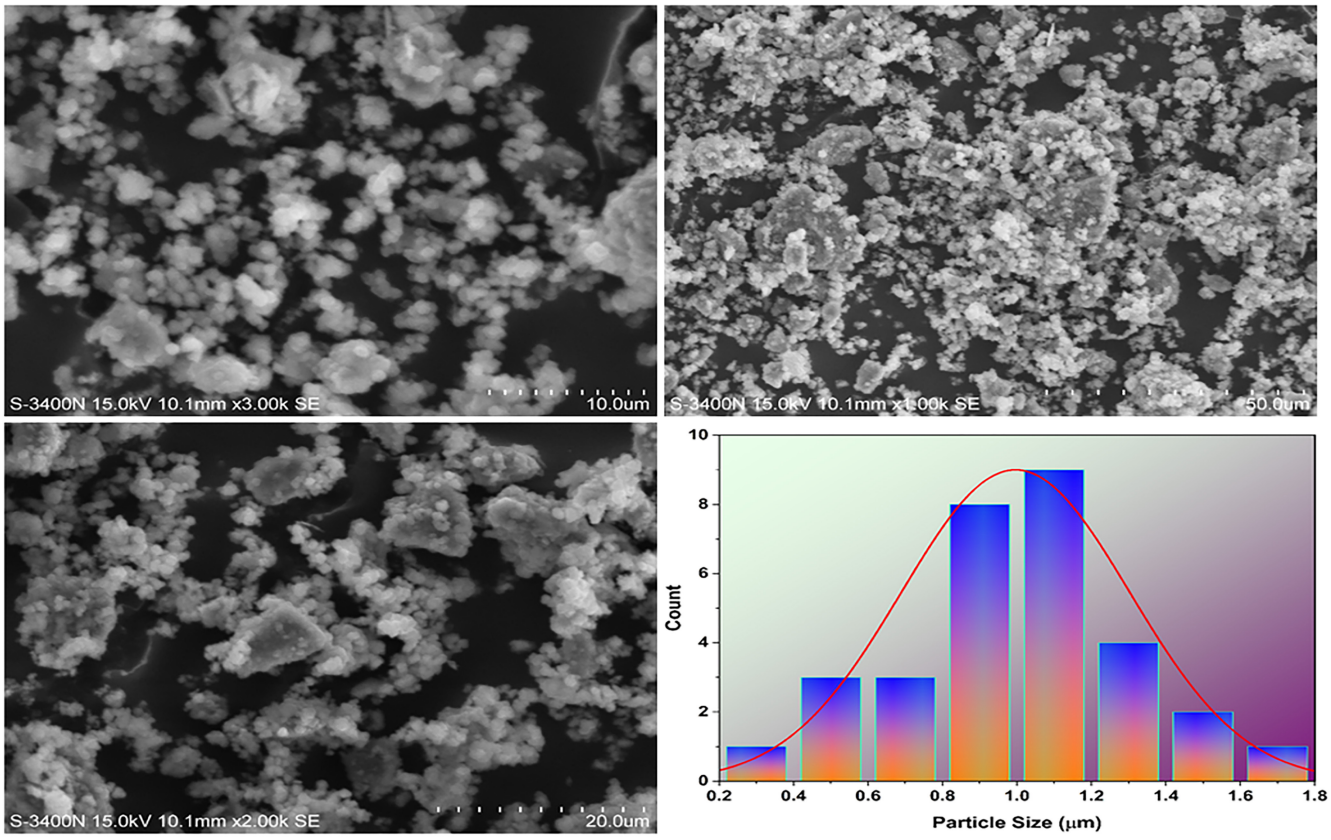

FIGURE 4 | SEM image of $Ca_{10}(PO_4)_6Cl_2$ phosphor.

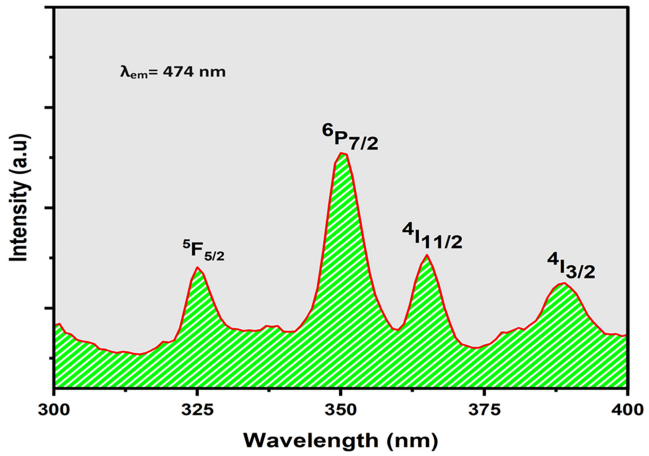

FIGURE 5 | Excitation spectrum of $Ca_{10}(PO_4)_6Cl_2$:Dy^{3+} phosphor.

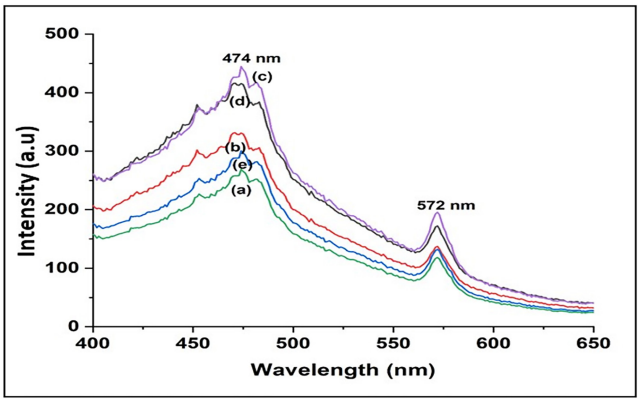

FIGURE 6 | Emission spectrum of $Ca_{10}(PO_4)_6Cl_2$: Dy^{3+} phosphor: (a) $Dy^{3+}=0.5$ mol%, (b) $Dy^{3+}=1.0$ mol%, (c) $Dy^{3+}=1.5$ mol%, (d) $Dy^{3+}=2$ mol%, and (e) $Dy^{3+}=2.5$ mol%.

that the prepared phosphor material efficiently exited by near-ultraviolet light. The photoluminescence emission spectra of various of Dy^{3+} ions activated $Ca_{10}(PO_4)_6Cl_2$ phosphor display in Figure 6, which recorded at constant excitation wavelength at 350 nm. It observed that the luminescence emission spectrum is in 400 to 650 nm range of wavelength. Photoluminescence emission spectra contain two strong intense peaks positioned at 474 and 572 nm wavelength. In emission spectra, peak located at 474 nm ascribe due to the transition from exited state $^4F_{9/2}$ to ground $^6H_{15/2}$ and emission band at 572 corresponds to transition $^4F_{9/2}\rightarrow{}^6H_{13/2}$ of Dy^{3+} ions [29, 30]. Out of these two strong peaks, the peak located at 474 nm was high-intensity peak than peak located at 572 nm. The blue color emitted at $^4F_{9/2}\rightarrow{}^6H_{15/2}$ (474 nm) is MD transition with selection rule $\Delta J=0, \pm1$ which varies with environment around Dy^{3+} ions. Yellow color emission because of transition $^4F_{9/2}\rightarrow{}^6H_{13/2}$ (572 nm) is forced ED transition with rule of selection, $\Delta J=0, \pm2$, which strongly influence with field strength present in the rare earth ion. The 472 nm ($^4F_{9/2}\rightarrow{}^6H_{15/2}$) is maximum intensity peak in the emission spectra occupied inversion symmetric site. In this work, the MD transition is highly prominent than ED transition. Figure 7 shows the variation of activator Dy^{3+} in concentration was affected on the luminescence intensity of $Ca_{10}(PO_4)_6Cl_2$ phosphor. The luminescence emission intensity rises as activator concentration Dy^{3+} ion increases from 0.5 up to 1.5 mol%., after that, the luminescence emission intensity decreases as the concentration of dopont ions increases. From this result, it is concluded that the interaction between the neighboring atoms is negligible at lower concentrationtherefore, the intensity increases as the concentration increases, and for higher concentration, the nearest atoms are interacting with each other and the distance between nearest ions decreases; this is because of the non-radiative (NR) coupling between the two dysprocium ions because of the mechanism of concentration quenching.

The Blasse's theory proposed the R_C (critical distance) determined by utilizing the following equation [23],

$$R_c \approx 2\left(\frac{3V}{4\pi NX_c}\right)^{\frac{1}{3}} \quad (1)$$

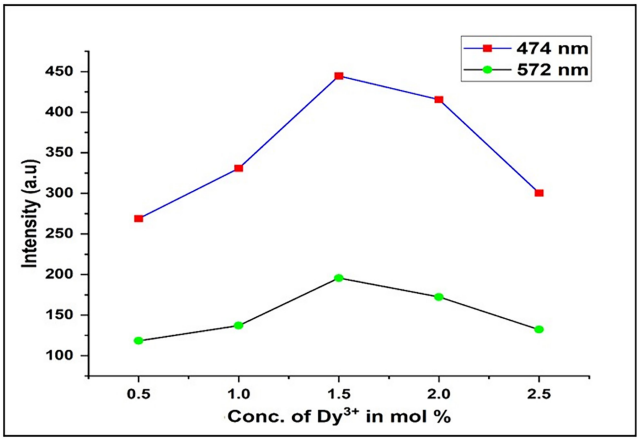

FIGURE 7 | Effect of Tb^{3+} concentration on emission intensity at 474and 572 nm.

where V stands for the volume of unit cell for $Ca_{10}(PO_4)_6Cl_2$, X_C is concentration reached to maximum value of intensity ($X_C=0.015$), and N represents the number of the activator ($N=1$). In the current study, $V=538.96$ Å. By putting all the values, the value between Dy^{3+}–Dy^{3+} ions of critical distance (R_C) was calculated as 40.947 Å with $X_C=0.015$. The calculated R_C value more than 5 Å; it shows that the mechanism concentration quenching is primarily caused by electronic multipole interactions. To more specifically analyze the type of interaction, we associate the photoluminescence intensity with the concentration of Dy^{3+} ions based upon theory reported by Van vitert. The relation between the dopant and the photo-luminescence intensity can be determined by using the following formula

$$\frac{I}{X} = K\left[1+\beta(X)^{\frac{Q}{3}}\right]^{-1} \quad (2)$$

In these relation, I represents the intensity of the material. X is the molar concentration of Sm^{3+} ions, β and K are constants; the values of Q show index electric multipole. The value of Q is equal

to 3; then, the interaction is migration of energy between nearest ions. The value of Q equals to 6, 8, and 10; then, the interaction of transfer of energy is due to multiple–multiple interaction. For dipole–dipole interaction, the Q value is 6; for dipole–quadrupole, the Q value is 8; and for quadrupole–quadrupole interaction, Q is 10. The value of Q can be determined by the slope between log (I/x) and log(x) is ($-Q/3$). This phenomenon was further investigated using emission spectra at a wavelength of 474 and 572 nm, by utilizing Dexter's theory, the slope of curve is −1.74 and −1.75, respectively, as displayed in Figure 8. In Equation (2), the value of θ is about 5.22 (447 nm) and 5.25 (572 nm), which is very close to 6. The obtained value of critical distance and the value of Q indicate that the effect of concentration quenching in between the neighboring ions is attributed due to dipole–dipole interaction [31].

3.6 | Photoluminescence Properties of Tb^{3+} Doped $Ca_{10}(PO_4)_6Cl_2$ Phosphor

The photoluminescence studies involve the investigation of the emission of light from material after it has absorbed photons; these are crucible for understanding the electronic and optical properties of materials. The luminescence absorption and emission spectrum of Tb^{3+} activated $Ca_{10}(PO_4)_6Cl_2$ phosphor

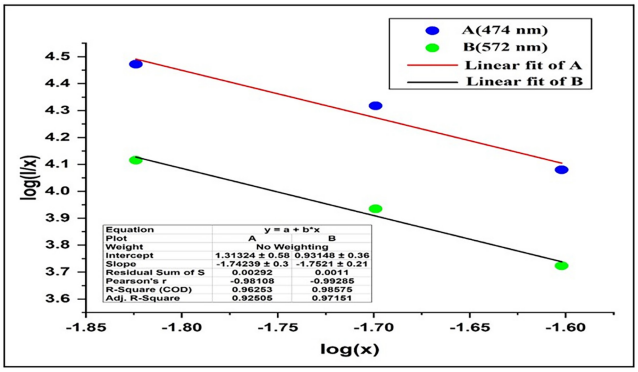

FIGURE 8 | Graph of $Ca_{10}(PO_4)_6Cl_2$:Dy^{3+} phosphor log (x) vs log (I/x) with fitting curve.

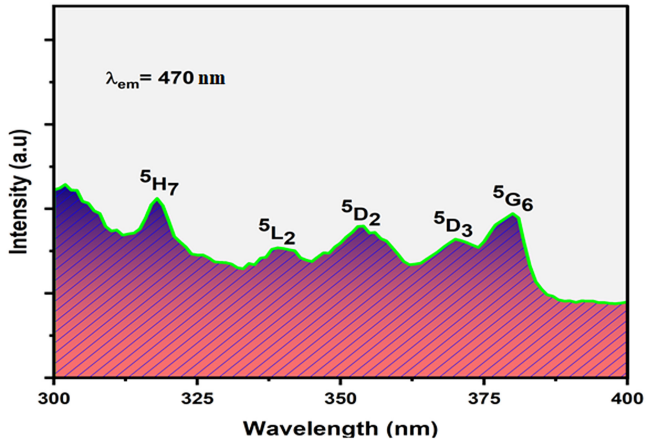

FIGURE 9 | Excitation spectrum of $Ca_{10}(PO_4)_6Cl_2$: Tb^{3+} phosphor.

synthesized by the wet-chemical method was analyzed at normal temperature. Figure 9 reveals the photoluminescence excitation spectra of $Ca_{10}(PO_4)_6Cl_2$:Tb^{3+} phosphor monitored for emission wavelength 470 nm, which has many excited levels ranging in the 300- to 400-nm wavelength. The excited lines are positioned at 317, 339, 354, 371, and 379 nm. All these peaks belong to the 4f-4f transition of Tb^{3+} ions, which corresponds to the ground state $^7F_6$ to different excited states $^5H_7$, $^5L_2$, $^5D_2$, $^5D_3$, and $^5G_6$ transitions of Tb^{3+} ions, respectively [32]. Among all these bands, the strongest excitation peak is centered at 379 nm, making it ideal for measuring the photoluminescence (PL) emission spectra.

The PL emission spectrum of $Ca_{10}(PO_4)_6Cl_2$:Tb^{3+} phosphor of various concentrations was excited at wavelengths 379 and 354 nm shown in Figure 10. The PLE spectra contain two main characteristic peaks in the 425–575-nm region of Tb^{3+} ions. These two emission peaks are located at 470 and 543 nm. The emission peaks at 470 and 543 nm are attributed to $^5D_4 \rightarrow {}^7F_6$ and $^5D_4 \rightarrow {}^7F_5$ transitions of Tb^{3+} ions [33, 34]. PL emission spectra of Tb^{3+} in $Ca_{10}(PO_4)_6Cl_2$ phosphor exhibit the blue color at 470 nm and green color at 543 nm. Figure 5 shows two emission spectra of the same nature and peaks observed at the same wavelengths at different wavelengths measured under 354 and 379 nm. From these two peaks, the highest intensity peak is found at 470 nm wavelength. The $^5D_4 \rightarrow {}^7F_6$ (470) transition of the terbium ion is an ED transition, and the $^5D_4 \rightarrow {}^7F_5$ transition is an allowed induced ED transition, following the selection rule $\Delta J = 2$. The ED transition is more intensive than the other. The most intense peak is observed at 1.5 mol% for both emission spectra excited at 379 and 354 nm. All results show that $Ca_{10}(PO_4)_6Cl_2$:Tb^{3+} phosphor is suitable for green emission display devices and solid-state lighting applications.

The emission intensity of the material changes with various amounts of Tb^{3+} ions represented in Figure 11. From Figure 11, it was observed that increasing the Tb^{3+} ion concentration from 0.5 to 1.5 mol% led to an increase in emission intensity. However, beyond 1.5 mol%, the emission intensity began to decrease. This decrease can be explained by a phenomenon called concentration quenching, where so many Tb^{3+} ions start transferring energy among themselves instead of emitting light [35]. At 1.5 mol% concentration, the maximum emission intensity was found, and at higher concentrations, too much energy transfer and interaction caused processes that do not emit light to become dominant. This led to a fall in emission intensity.

Using the method explained in Equation (1), critical distance (RC) was calculated to be 40.947 Å for $X_C = 0.015$. Because this value is greater than 5 Å, concentration quenching is likely due to electronic multipole interactions. To investigate this mechanism, emission spectra at 470 and 543 nm were analyzed. Based on Dexter's theory, the slopes of the curves were found to be −1.26 at 470 nm and −1.22 at 543 nm, as shown in Figure 12. Using Equation (2), the Q values were calculated as approximately 3.78 and 3.66, which are close to 6. This indicates that the concentration quenching between Tb^{3+}–Tb^{3+} ions mainly occurs through dipole–dipole interactions [36].

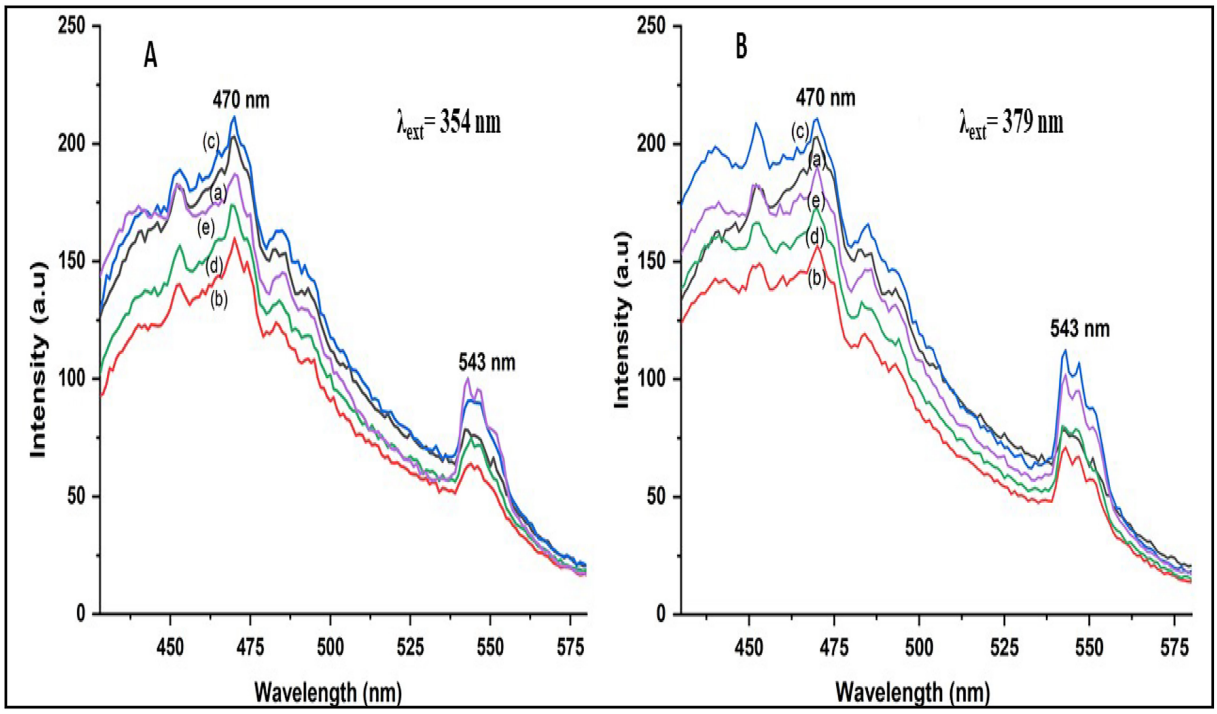

FIGURE 10 | Emission spectrum of $Ca_{10}(PO_4)_6Cl_2$:Tb^{3+} phosphor: (a) $Tb^{3+} = 0.5$ mol%, (b) $Tb^{3+} = 1$ mol%, (c) $Tb^{3+} = 1.5$ mol%, (d) $Tb^{3+} = 2.0$ mol%, and (e) $Tb^{3+} = 2.5$ mol%.

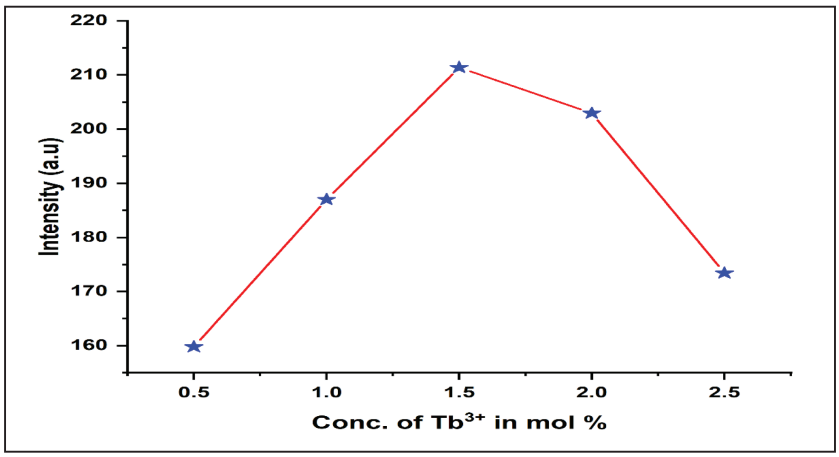

FIGURE 11 | Effect of Tb^{3+} concentration on emission intensity at 470 nm.

3.7 | Energy Level Diagram $Ca_{10}(PO_4)_6Cl_2$:Dy^{3+} and Tb^{3+} Phosphors

The schematic $Ca_{10}(PO_4)_6Cl_2$:Dy^{3+} phosphor energy level diagram with possible excitation and emission wavelengths with cross relaxation channels of Dy^{3+} ions in $Ca_{10}(PO_4)_6Cl_2$ host material are presented in Figure 13. Under the constant excitation at 350 nm, the electron in $^6H_{15/2}$ ground state will absorb the excited energy, and it moves to the excited states by resonance process. After that, this absorbed energy is transferred to the Dy^{3+} ions and populated in the energy level $^6H_{15/2}$. Various excitation wavelengths of Dy^{3+} ions located at 325, 350, 365, and 389 nm, the Dy^{3+} ions excited from the lower energy level $^6H_{15/2}$ to move to different excited energy level like $^4F_{5/2}$, $^6P_{7/2}$, $^6P_{5/2}$, and $^4F_{7/2}$. From all these different excited levels, the electron relaxes to the lower state of excited energy state, that is, $^4F_{9/2}$ of Dy^{3+} ions via the process of NR relaxation, and again, the electron populates from the $^4F_{9/2}$ energy level and comes back or returns to different lower energy states $^6H_{15/2}$, and $^6H_{13/2}$ gives blue and yellow emission [37].

The schematical energy level diagram of Tb^{3+} ions doped in $Ca_{10}(PO_4)_6Cl_2$ phosphor under the constant excitation at 379 nm is shown in Figure 14. Electrons of Tb^{3+} ions absorb energy and become excited; then, they jump from the ground energy to higher energy levels, that is, $^7F_5$ to $^4F_{5/2}$, $^6P_{7/2}$, $^6P_{5/2}$, $^4F_{7/2}$, and $^4F_{9/2}$ at 317, 339, 354, 371, and 379 nm, respectively. Initially, the electrons relax to the lowest energy level of excited level $^5D_4$ via

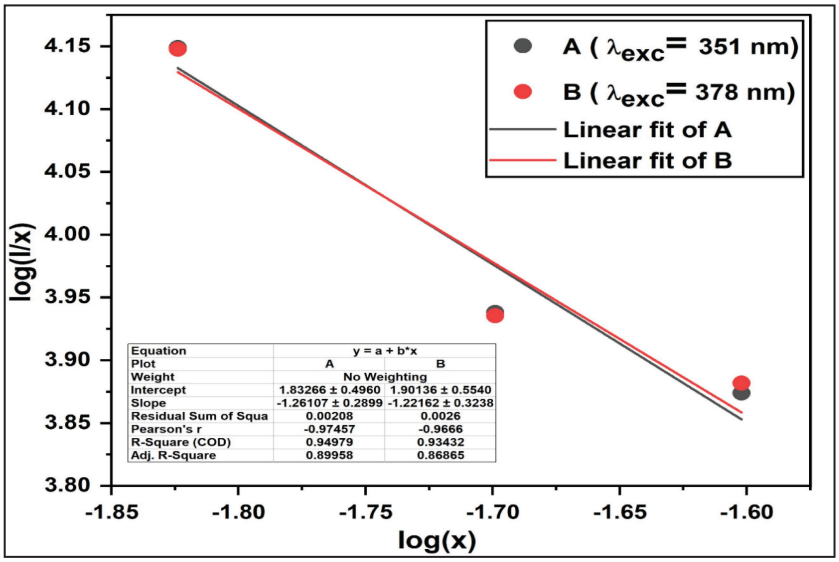

FIGURE 12 | Graph of $Ca_{10}(PO_4)_6Cl_2:Tb^{3+}$ phosphor log (x) vs log (I/x) with fitting curve.

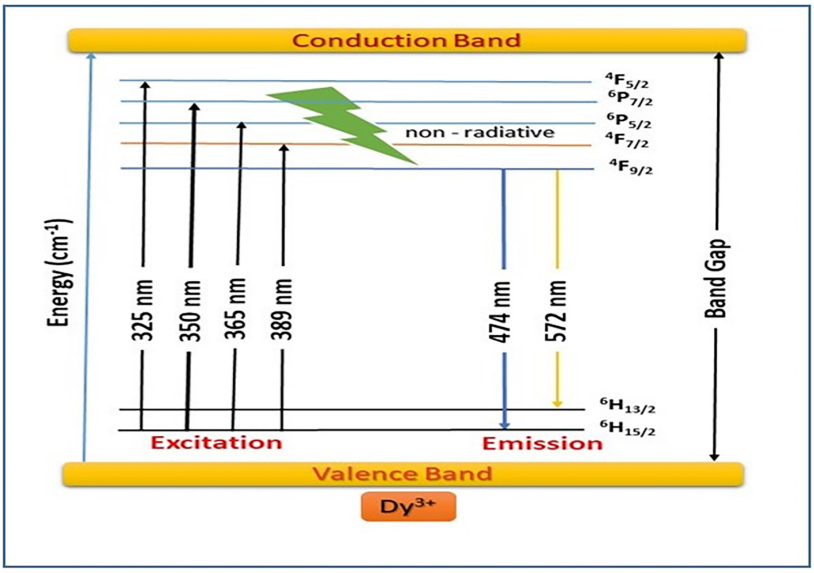

FIGURE 13 | Energy level diagram of $Ca_{10}(PO_4)_6Cl_2:Dy^{3+}$ phosphor.

NR transition. This is because of the energy difference between levels or states. Finally, the electron from $^5D_4$ electronic states falls down to the lower energy levels $^5D_4 \rightarrow {}^7F_5$ at 470 nm and $^5D_4 \rightarrow {}^7F_6$ at 543 nm by emitting a photon, which emits blue and green emission of light [38].

3.8 | Chromatic Properties of $Ca_{10}(PO_4)_6Cl_2:Dy^{3+}$ and Tb^{3+} Phosphors

The CIE chromaticity is a method to describe and measure color based on how humans perceive it. It is crucial in color science and used to determine the color purity of light emitted by materials like phosphors. The most intense emission spectrum was used to record the coordinates of the prepared phosphor material. The color coordinate (CIE) of highly intense concentration of Dy^{3+}-activated $Ca_{10}(PO_4)_6Cl_2$ phosphor is detected (0.112, 0.097) at 474 nm and (0.458, 0.40) at 572 nm in Figure 15A [39]. These color coordinates lie on blue and green-yellow boundary of color chromaticity picture. The color chromaticity diagram of Tb^{3+}-doped $Ca_{10}(PO_4)_6Cl_2$ phosphor is represented in Figure 15B. The color chromatic point of Tb^{3+}-activated $Ca_{10}(PO_4)_6Cl_2$ phosphor lies in the border of blue region at 470 nm and green region at 543 nm of CIE diagram. The calculated color CIE coordinate of Tb^{3+}-activated $Ca_{10}(PO_4)_6Cl_2$ phosphor are found to be (0.124, 0.0577) at 470 nm and (0.251, 0.736) at 543 nm; it shows the that synthesized phosphors have high color purity [40]. All these color coordinates show the given phosphor materials, which have high color purity, so it indicates that the synthesized phosphor materials are potential candidate for blue and green emitting lighting WLED application.

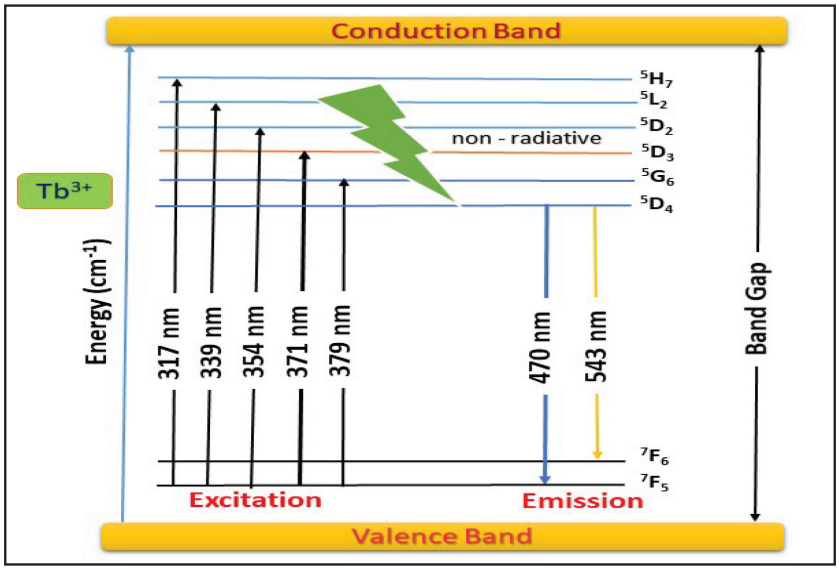

FIGURE 14 | Energy level diagram of $Ca_{10}(PO_4)_6Cl_2$:Tb^{3+} phosphor.

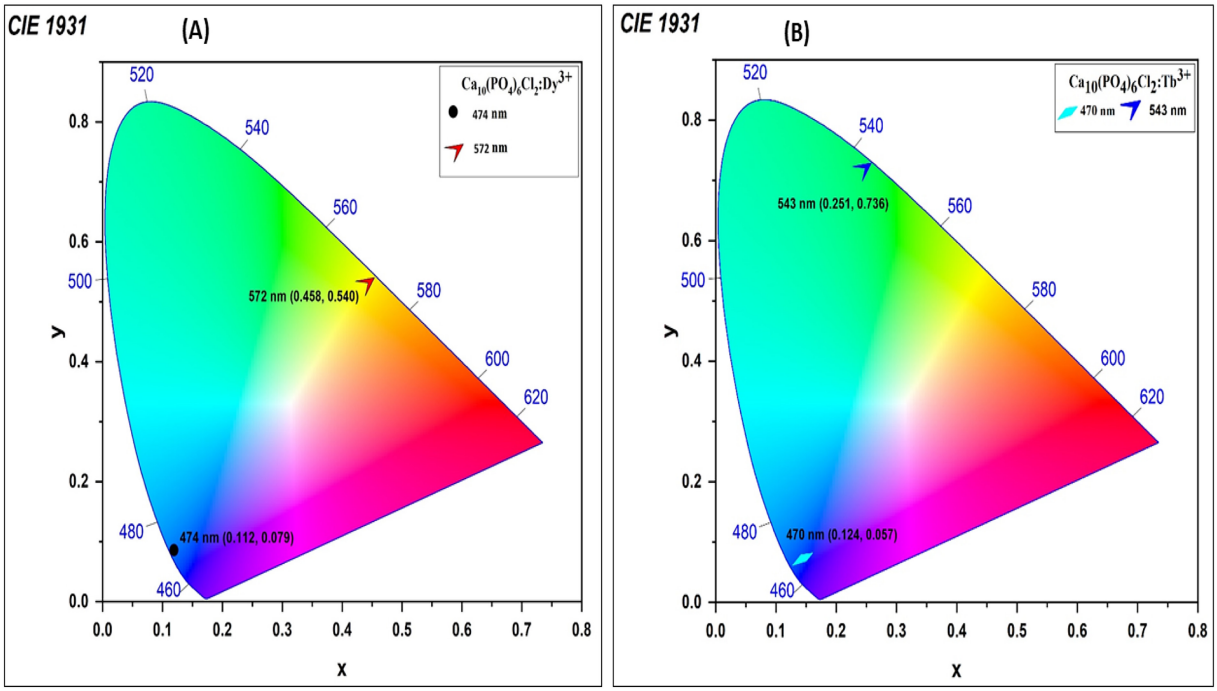

FIGURE 15 | Chromaticity diagram of $Ca_{10}(PO_4)_6Cl_2$:Dy^{3+} and Tb^{3+} phosphors.

4 | Conclusion

The different concentrations of Dy^{3+}- and Tb^{3+}-activated $Ca_{10}(PO_4)_6Cl_2$ phosphors have been prepared by the wet chemical technique. The structural, morphological, and optical studies of the prepared phosphor were studied by using SEM, FTIR, photoluminescence spectra, and CIE color coordinates. The crystal structure of synthesized $Ca_{10}(PO_4)_6Cl_2$ phosphor exhibits the hexagonal structure with the P 63/m space group. The FTIR spectra of $Ca_{10}(PO_4)_6Cl_2$ phosphor contain various types of chemical bonds including P-O, Ca-O, and O-H bonds and confirm the presence of the phosphate $(PO_4)^{3-}$groups. The SEM image of synthesized $Ca_{10}(PO_4)_6Cl_2$ phosphor shows the particle size ranges in several micrometers. The size of the particle is non-uniform in size and shape. The photoluminescence (PL) study of the produced $Ca_{10}(PO_4)_6Cl_2$:Dy^{3+} phosphor exhibits two emission peaks located at 474 and 572 nm, producing blue and yellow colors. These emissions arise from the $^4F_{9/2} \rightarrow {}^6H_{15/2}$ and $^6H_{13/2}$ transitions of Dy^{3+} ions, respectively, under excitation at 350 nm. The high-intensity peak is observed at 474 nm. The maximum concentration of Dy^{3+} ions is 1.5 mol%. The PLE spectra of $Ca_{10}(PO_4)_6Cl_2$:Tb^{3+} contain two main characteristic emission peaks placed at 470 (blue) nm and 543 (green) nm corresponding to $^5D_4 \rightarrow {}^7F_6$ and $^5D_4 \rightarrow {}^7F_5$ of Tb^{3+} ions monitored by

354 and 379 nm excitation. The most intense peak is at 470 nm. The high intense band is obtained at 1.5 mol% concentration of Tb^{3+} ions. The calculated value of critical distance is 40.947 Å, and $Q = 5.22$ (447 nm) and 5.25 (572 nm) by using Dexter theory concentration quenching between Dy^{3+} ions is attributed to dipole–dipole interactions. The critical distance (R_C) is 40.947 Å ($X_C = 0.015$) by applying Dexter's theory; the value of Q was found to be 3.78 and 3.3.66, which is very close to 6. This reveals that the concentration quenching mechanism between the Tb^{3+}–Tb^{3+} ions is primarily attributed to dipole–dipole interactions. The color coordinates of highly intense concentration of Dy^{3+}-activated $Ca_{10}(PO_4)_6Cl_2$ phosphor are detected to be (0.112, 0.097) at 474 nm and (0.458, 0.40) at 572 nm; these color CIE coordinates lie in the region of blue and green-yellow at the edge of the CIE diagram. The color chromatic point of Tb^{3+}-activated $Ca_{10}(PO_4)_6Cl_2$ phosphor lies in the border of blue region at 470 nm and green region at 543 nm with color coordinates (0.124, 0.0577) and (0.251, 0.736) of CIE diagram, respectively. Based on the extensive research conducted, the synthesized phosphors demonstrate significant possibilities for use in lighting technologies.

Conflicts of Interest

The authors declare no conflicts of interest.

Data Availability Statement

The data that support the findings of this study are available from the corresponding author upon reasonable request.

References

1. Y. Li, M. Gecevicius, and J. Qiu, "Long Persistent Phosphors—From Fundamentals to Applications," *Chemical Society Reviews* 45, no. 8 (2016): 2090–2136.

2. R. T. Maske, A. N. Yerpude, R. S. Wandhare, A. Nande, and S. J. Dhoblez, "Combustion Synthesized Novel $SrAlBO_4$: Eu^{3+} Phosphor: Structural, Luminescence, and Judd-Ofelt Analysis," *Optical Materials* 141 (2023): 113893.

3. J. Cho, J. H. Park, J. K. Kim, and E. F. Schubert, "White Light-Emitting Diodes: History, Progress, and Future," *Laser & Photonics Reviews* 11, no. 2 (2017): 1600147.

4. M. H. Fang, Z. Bao, W. T. Huang, and R. S. Liu, "Evolutionary Generation of Phosphor Materials and Their Progress in Future Applications for Light-Emitting Diodes," *Chem. Rev.* 122, no. 13 (2022): 11474–11513.

5. G. B. Nair, H. C. Swart, and S. J. Dhoble, "A Review on the Advancements in Phosphor-Converted Light Emitting Diodes (pc-LEDs): Phosphor Synthesis, Device Fabrication and Characterization," *Progress in Materials Science* 109 (2020): 100622.

6. I. Gupta, S. Singh, S. Bhagwan, and D. Singh, "Rare Earth (RE) Doped Phosphors and Their Emerging Applications: A Review," *Ceramics International* 47, no. 14 (2021): 1–9282.

7. X. Song, M. H. Chang, and M. Pecht, "Rare-Earth Elements in Lighting and Optical Applications and Their Recycling," *JOM* 65 (2013): 1276–1282.

8. R. T. Maske, A. N. Yerpude, R. S. Wandhare, and S. J. Dhoble, "Photoluminescence Studies of SrAlBO4: RE3+ (RE3+ = Dy^{3+} and Sm^{3+}) Phosphor Synthesized by Combustion Method for W-LEDs," *Journal of Optics* 53 (2024): 2384–2391.

9. B. Bawanthade, A. Mistry, and S. J. Dhoble, "Study of Optical Properties of Sr10(PO4)6F2 Apatite Kind Phosphor Prepared by Co-precipitation Method for W-LED Applications," *Journal of Materials Science: Materials in Electronics* 35, no. 18 (2024): 1259.

10. N. C. George, K. A. Denault, and R. Seshadri, "Phosphors for Solid-State White Lighting," *Annual Review of Materials Research* 43, no. 1 (2013): 481–501.

11. S. R. Bhelave, A. N. Yerpude, and S. J. Dhoble, "Comparative Photoluminescence Study of MAlB3O7: Dy^{3+} (M=Ca, Sr) Phosphor for Solid-State Lighting Applications," *Journal of Optics* 53, no. 2 (2024): 1050–1057.

12. R. T. Maske, A. N. Yerpude, K. N. Shinde, R. S. Wandhare, and S. J. Dhoble, "Combustion Synthesis of Sr2Al2B2O8:RE (RE = Dy^{3+}, Eu^{3+}, Sm^{3+}) Phosphor for Solid-State Lightning Application," *Journal of Optics* 53 (2023): 3666–3676.

13. R. Shrivastava, J. Kaur, and V. Dubey, "White Light Emission by Dy^{3+} Doped Phosphor Matrices: A Short Review," *Journal of Fluorescence* 26 (2016): 105–111.

14. C. M. Nandanwar, N. S. Kokode, A. N. Yerpude, R. M. Yerojwar, and S. K. Sayyad, "Wet Chemical Synthesis and Photoluminescence Properties of NaSrPO4:Dy^{3+} and NaSrPO4:Eu^{3+} Phosphors for Near UV-Based w-LEDs," *Journal of Optics* 53 (2023): 1764–1770.

15. S. K. Ramteke, A. N. Yerpude, N. S. Kokode, and S. J. Dhoble, "Optical Properties of Rare Earth-Activated Ca3(PO4)2:RE (RE = Eu^{3+} and Dy^{3+}) Phosphors Prepared by Wet Chemical Synthesis," *Bulletin of Materials Science* 44, no. 3 (2021): 174.

16. S. Maurya, S. Kumari, P. Rohill, A. Prasad, and A. S. Rao, "Dy^{3+} Doped $KCa(PO_3)_3$ Phosphor for White Light Generation: Structural and Luminescent Studies," *Physica Scripta* 99, no. 6 (2024): 065573.

17. Y. R. Parauha and S. J. Dhoble, "Structural and Photoluminescence Properties of Dy^{3+}-Activated NaCaPO4 Phosphor Derived From Solution Combustion," *Luminescence* 37, no. 1 (2022): 141–152.

18. D. M. Pimpalshende and S. J. Dhoble, "Synthesis And Luminescent Performance Of LaPO4: Dy Nanophosphor," *Advanced Materials Letters* 5, no. 12 (2014): 688–691.

19. P. Khajuria, M. Manhas, A. K. Bedyal, A. Vij, H. C. Swart, and V. Kumar, "Structural and Spectral Investigation of a Near-UV-Converted LiSrP3O9:Dy^{3+} Phosphor for White Light-Emitting Diodes," *Journal of Materials Science: Materials in Electronics* 33, no. 8 (2022): 6031–6042.

20. C. M. Nandanwar, N. S. Kokode, A. N. Yerpude, and S. J. Dhoble, "Combustion Synthesis of KZnPO4: RE (RE = Dy^{3+} and Sm^{3+}) Phosphors for n-UV Based w-LEDs," *European Physical Journal Applied Physics* 98 (2023): 50.

21. B. Ramesh, G. R. Dillip, B. Rambabu, S. W. Joo, and B. D. P. Raju, "Structural Studies of a Green-Emitting Terbium Doped Calcium Zinc Phosphate Phosphor," *Journal of Molecular Structure* 1155 (2018): 568–572.

22. C. M. Nandanwar, N. S. Kokode, A. N. Yerpude, and S. J. Dhoble, "Luminescence Properties of BiPO4:Ln (Ln = Dy^{3+}, Tb^{3+} and Sm^{3+}) Orthophosphate Phosphors for Bear-UV-Based Solid-State Lighting," *Bulletin of Materials Science* 46, no. 1 (2023): 51.

23. V. Singh, A. R. Kadam, S. J. Dhoble, and H. Jeong, "VUV and UV Photoluminescence of Green Emitting Sr2P2O7:Tb^{3+} Phosphors for PDP Applications," *Optik* 243 (2021): 167396.

24. B. V. Ratnam, M. Jayasimhadri, G. B. Kumar, et al., "Synthesis and Luminescent Features of NaCaPO4:Tb^{3+} Green Phosphor for Near UV-Based LEDs," *Journal of Alloys and Compounds* 564 (2013): 100–104.

25. R. T. Maske, A. N. Yerpude, and S. J. Dhoble, "Wet Chemical Synthesis of Sm^{3+} Doped Ca10(PO4)6Cl2 Phosphor for w-LED Application," *Materials Letters: X* 19 (2023): 100214.

26. S. Ye, F. Xiao, Y. X. Pan, Y. Y. Ma, and Q. Y. Zhang, "Phosphors in Phosphor-Converted White Light-Emitting Diodes: Recent Advances in Materials, Techniques and Properties," *Materials Science & Engineering R: Reports* 71 (2010): 1.

27. R. T. Maske, A. N. Yerpude, R. S. Wandhare, and S. J. Dhoble, "Photoluminescence Properties of Novel Ca3Al10O18:RE^{3+} (RE^{3+} = Dy^{3+}, Sm^{3+}) Phosphor Prepared via Combustion Synthesis for Solid-State Lightning Devices," *Journal of Materials Science: Materials in Electronics* 35, no. 26 (2024): 1728.

28. C. M. Nandanwar, R. M. Yerojwar, N. S. Kokode, A. N. Yerpude, and S. J. Dhoble, "Synthesis and photoluminescence properties of AlPO4:Ln (Ln = Dy^{3+}, Eu^{3+} and Sm^{3+}) Phosphors for Near UV-Based White LEDs Application," *Indian Journal of Physics* 98, no. 3 (2024): 1083–1093.

29. T. A. Lodi, N. F. Dantas, T. S. Gonçalves, A. S. S. de Camargo, and F. Pedrochi, "Dy^{3+} Doped Calcium Boroaluminate Glasses and Blue Led for Smart White Light Generation," *Journal of Luminescence* 207 (2019): 378.

30. R. T. Maske, A. N. Yerpude, R. S. Wandhare, and S. J. Dhoble, "Structural, Morphological, and Photoluminescence Properties of RE (RE = Dy^{3+}, Eu^{3+}, Sm^{3+})-Doped CaAlBO4 Phosphor Synthesized by Combustion Method," *Luminescence* 38, no. 10 (2023): 1814–1824.

31. S. S. Babu, P. Babu, C. K. Jayasankar, T. Tröster, W. Sievers, and G. Wortmann, "Optical Properties of Dy3+-Doped Phosphate and Fluorophosphate Glasses," *Optical Materials* 31, no. 4 (2009): 624–631.

32. M. Dahiya, A. Siwach, M. Dalal, and D. Kumar, "Study of Structural and Luminescent Characteristics of Novel Color Tunable Blue-Green Tb^{3+}-Doped Na3Y(PO4)2 Nanoparticles for NUV-Based WLEDs," *Journal of Materials Science: Materials in Electronics* 32 (2021): 4166–4176.

33. J. Cheng, X. Bian, Z. Zhai, M. Sardar, and J. Lu, "A Single-Phase Full-Color Phosphor Sr2Ca2La(PO4)3O:Eu^{2+},Tb^{3+},Mn^{2+}: Photoluminescence and Energy Transfer," *Journal of Rare Earths* 40, no. 4 (2022): 541–550.

34. C. C. Lin, Y. S. Tang, S. F. Hu, and R. S. Liu, "KBaPO4:Ln (Ln=Eu, Tb, Sm) Phosphors for UV Excitable White Light-Emitting Diodes," *Journal of Luminescence* 129, no. 12 (2009): 1682–1684.

35. P. Gupta, A. K. Bedyal, V. Kumar, et al., "Photoluminescence and Thermoluminescence Properties of Tb 3+ Doped K 3 Gd(PO4) 2 Nanophosphor," *Materials Research Bulletin* 60 (2014): 401–411.

36. K. Jha, A. K. Vishwakarma, M. Jayasimhadri, and D. J. Haranath, "Multicolor and White Light Emitting Tb^{3+} /Sm^{3+} Co-Doped Zinc Phosphate Barium Titanate Glasses via Energy Transfer for Optoelectronic Device Applications," *Journal of Alloys and Compounds* 719 (2017): 116–124.

37. A. R. Beck, S. Das, and J. Manam, "Temperature Dependent Photoluminescence of Dy^{3+} Doped $LiCaBO_3$ Phosphor," *Journal of Materials Science: Materials in Electronics* 28, no. 1 (2017): 17168–17676.

38. A. A. da Silva, M. A. Cebim, and M. R. Davolos, "Excitation Mechanisms and Effects of Dopant Concentration in Gd2O2S:Tb^{3+} Phosphor," *Journal of Luminescence* 128, no. 7 (2008): 1165–1168.

39. H. J. Rajendra, C. Pandurangappa, and D. L. Monika, "Luminescence Properties of Dysprosium Doped YVO4 Phosphor," *Journal of Rare Earths* 36, no. 12 (2018): 1245–1249.

40. R. T. Maske, A. N. Yerpude, R. S. Wandhare, V. Chopra, and S. J. Dhoble, "Structural, Morphological and Photoluminescence Studies of Ca7Mg2P6O24:RE^{3+}(RE^{3+}= Tb^{3+}, Dy^{3+}) Nanophosphor for Solid State Illumination," *Chemical Physics Impact* 9 (2024): 100760.